Rupture Dynamics in Model Polymer System with Catch Bonds

A DISSERTATION

Submitted in partial fulfillment of the requirements for the award of

the degree of

Master of Technology

in

Advanced Chemical Analysis

By

SHIVAM GUPTA

(17549006)

DEPARTMENT OF CHEMISTY

INDIAN INSTITUTE OF TECHNOLOGY ROORKEE

ROORKEE-247667

June 2019

Candidate's Declaration

I hereby declare that my work, which is being presented in this dissertation entitled "**Rupture Dynamics in Model Polymer System with Catch Bonds**", submitted in partial fulfillment of requirement for the award of the degree of "**Master of Technology (Advanced Chemical Analysis)"** and submitted to the Department of Chemistry, Indian Institute of Technology, Roorkee is an authentic work done by me, under the guidance of **Dr. Pallavi Debnath**, Assistant Professor, Department of Chemistry, Indian Institute of Technology, Roorkee.

Date: June 10, 2019 **Shivam Gupta**

Place: IIT Roorkee (17549006**)**

Certificate

This is to certify that Mr. Shivam Gupta has completed the dissertation entitled **"Rupture Dynamics in Model Polymer System with Catch Bonds"** under my supervision. The above statement made by the candidate is correct to the best of my knowledge.

Dr. Pallavi Debnath

Assistant Professor

Department of Chemistry

IIT Roorkee

Acknowledgement

It gives me immense pleasure to express my sincere appreciation and gratitude to Dr. Pallavi Debnath for her constant encouragement, excellent guidance, patience and care during the entire course of M. Tech. dissertation. I also remain indebted for her understanding and support during the times when I was really down and depressed.

I express my sincere regards to the past and the present heads of department: Prof. M. R. Maurya and Prof. K. R. Justin Thomas and our M. Tech. coordinator Dr. Tapas Kumar Mandal.

I am grateful to Indian Institute of Technology Roorkee for giving me an opportunity to pursue M. Tech. at the Department of Chemistry and providing me with the financial support (Institute assistantship). I would also like to thank the office staff of our department for their kind cooperation.

I would like to thank my office-mates: Prakhar, Neha and Garima for making our office a lively, exciting place to work for hours together and special thanks to Mr. Nabi Ahamad for being thoughtful and generous throughout and encouraging me to do my best.

My deepest gratitude goes to my sister Raunak Gupta for her unflagging love and unconditional support throughout my life and my studies.

I would like to thank everybody who were important to the successful realization of thesis, and at the same time, express my apology that I could not mention them personally one by one.

Shivam Gupta

Abstract

In this thesis, I investigate the rupture dynamics of a generic model polymer system involving interconnecting catch bonds (rather than a slip bond) between a rigid and a flexible transducer, where a constant force is applied to the latter. The aim is to study microscopic mechanism due to relative movement of (soft) surfaces at single polymer level with these new catch bonds which are allowed to rupture only, stochastically. I simulate the coupled equations of motion for bead and bond dynamics and develop a mean field formalism to gain further analytical insights. I provide my initial attempt to solve these analytical coupled mean-field equations under specific approximations.

Table of contents

List of Tables

List of Figures

Nomenclature

Abbreviation

n	Number of bead
γ	Coefficient of friction
k_T	Stiffness of polymeric transducer
F_T	Constant force applied on zeroth bond
δ	Dirac – delta function
k_0	Force free rate constant
$k_{-,n}$	Rupture rate
f_b	Critical force
α	Constant related to deformation energy
f_0	Saturation force
k_b	Stiffness of interconnecting bonds
θ	Heaviside step function
Δt	Time step
α_n	Random variable belong to (0, 1)
x_n	Displacement of bead
q_n	Bond variable

Chapter: 1

Introduction

Extensive studies had been performed over the years in underpinning the molecular mechanism underlying the phenomena involving relative motion between surfaces, in processes spanning over various disciplines in biology, for instance cellular processes, soft condensed mater physics, for example bio composites, complex fluids, and tribology like friction, to name a few. The models used to address these are generic and often raises questions about the general application of associated mechanism at molecular level. However the tractability (both analytical (mainly) and also numerical, and agreement of the resulting treatment with experimental observations are remarkable. Similar questions are addressed with a generic model polymer system.

Numerous attempts have been made in understanding the origin of different physical phenomenon at microscopic level that involves relative motion between shearing surfaces [1-2]. Examples of such phenomenon are frictional forces, hierarchical structures in bio composites having relative motion at each level of hierarchy, adhesive bonds between ligands and biological receptors [3].

Frictional force is a physical phenomenon of extreme practical importance, which involves relative motion between surfaces [4]. New experimental procedures have been reported that help in understanding relation between frictional forces and the microscopic properties of systems, so that friction at nanometer length scale can be investigated in detail. A range of such processes involving friction at microscopic level comes under the branch of nanotribology [5]. Recent studies that showed interest in friction have unveiled a broad spectrum of phenomenon and their new behavior few of them are static and kinetic friction forces, frictional aging, transition to sliding but it has only revived old concepts and still a lot needs to be done to gain insights at microscopic level. Experimental observations in nanoscale molecular systems provides intriguing structural as well as dynamical features of systems confined to two atomically smooth solid surfaces which motivated efforts in theoretical perspective either numerically or analytically.

In field of microscopic mechanism for frictional phenomena pioneering contribution is made by Schallamach [6] through his research on friction between rubber and the track assuming dynamic friction arise from the shearing and consequent breaking of different bonds between the rubbing members, and eventually a general equation was derived for the frictional force involving average life and the number of the bonds along with the average time lag between breaking and again remaking of a bond at a particular location. In a particular case of a perfectly smooth substrate, the friction accounts due to local stick slip happening at the sliding interface. Hence a molecular mechanism was proposed for the local stick slip phenomena, in which surface of a rubber polymer chain sticks to the interface of the moving surface, expands, detaches, relaxes and then again reattaches to repeat the cycle. In each cycle, stored energy during expansion in the polymer chain gets dissipated during the detachment and relaxation period in the form of heat and this is marked to be the origin of friction at macroscopic level. This spearheading work prompted various theorists working on different distinctions of the toy rupture model to understand the microscopic origin of the mechanism of friction. A remarkable work on this phenomena is done by Filippov and coworkers [1], they put forward a microscopic model that exhibits a relationship between the dynamics of rupture and formation of particular bond and macroscopic phenomena of friction. Here they include strongly nonlinear rupture effects that contributed mainly to energy dissipation which is beyond the elastic phase of the given system. Their model comprises two rigid plates attached by bonds that break spontaneously and then reform as they come in contact [7].

Many models exist resembling same features as pioneering Burridge Knopoff spring and box model and its modification in earthquake dynamics, it consists of an array of blocks in one dimension coupled by horizontal springs moving on a frictional surface [37]. This one dimensional setup is attached by other set of springs (analogous to interconnecting bonds) to a driving bar moving side by side horizontally parallel at a constant velocity. Perrson et. al. [8] did calculations using these models to understand block substrate friction at microscopic level, but the microscopy in detail, its relationship to macroscopic motion of plate and the conclusions are all different.

Biomaterials like bone, lobster cuticle, wood, glass sponge, nacre are few hierarchical composite structures of proteins and minerals [9]. Complex hierarchical structure is found in

wood in terms of length scales it can be seen as a fiber composite, a functionally graded material or a honeycomb [10]. At the macroscopic level, it can be contemplated as a cellular solid, composed mainly of parallel hollow tubes that are wood cells. Cell wall is a composite of fiber made of cellulose microfibrils inserted into a matrix of lignin and hemicelluloses. The cellulose microfibrils present around the wood cells at an angle called micro fibril angle. Through the adjustment of the micro fibril angle it is possible to change the mechanical properties, ranging from high stiffness to more flexibility as angle increases, experiments based on deformation were performed by Keckes et al. During tensile loading mechanical properties unravel a stick slip mechanism at both cellular and tissue level [11]. Using experimental model the results of the irreversible distortion process are explained, in this process a soft resilient matrix transfer shear stresses among cellulose fibrils. Bone is also a hierarchical biomaterial which consists of hydroxyapatite, collagen, water and some non-collagenous proteins [12]. At microscopic level mineral platelets and collagen molecule combine forming mineralized collagen fibrils represented on a nanometer scale. On micrometer scale these fibrils gather to form fiber bundles, then these bundles arranged in lamellae of almost constant content of mineral in the trabeculae and osteons which makeup an organ (represented on centimeter scale). Osteons have cylindrical structures present in compact bones [13]. Improvements in manipulation techniques of single molecule has led to various studies on molecular structure as a basis for bone toughness, among them is Thompson et al. [14] who performed tests on bone indentation and on collagen fibers and inferred that sacrificial bonds are present in polymer of bones which protect the polymer backbone by dissipating energy, and the required time for reformation of these bonds corresponds to the bone recovery time in the indentation test suggests that may be these sacrificial bonds are responsible for toughness of bone [13]. Literatures contain phenomenological tension shear chain model to explain the mechanical characteristics of bone like bio-composites [15].

In force spectroscopy of ligand receptor bonds, study of cooperative transport by molecular motors and cell adhesion, major role is played by the subject that involves theoretical description of the dynamics of cooperative molecular bonds under load [16]. An important role is played by cell adhesion in their pathological and physiological functions such as growth, differentiation, migration and other multiple cell events [17]. Many complex structures with fixed ligand molecules are formed by receptors present on the surface of cell membranes that

enable the cell to sense mechanical environment outside the cell. These multi-receptor ligand bonds are known as adhesion cluster. The function of receptor ligand binding is to mechanically link the extracellular environments with cytoskeleton. These bindings are affected by cytoskeleton contraction, mechanical loading of blood flow and some other factors. With the help of these linkers, cells are capable of sensing and responding to their environment actively and passively as well. Hence, the effect of mechanical loading on biomechanical response of receptor ligand interactions is extensively explored. Although statistical description of each receptor ligand bond individually is well understood by now but the collective response of multiple molecular bonds can turn out to be complex. In experiments though ruptured single molecule bond normally cannot rebind but it can in case of bond clusters till all other bonds are intact.

During the past two decades various experiments have been conducted to investigate the forced dissociation event of single receptor ligand bonds, whose measurements are taken by means of optical and magnetic tweezers, bio-membrane force probes and atomic force microscopy [18]. This experimental advancement encouraged theoretical studies of the rupture of bond pairs under load variation. Kramer's time dependent description of rupture process indicate that the rupture strength depends on rate of loading [19]. Recent analytical formulations on dynamic stability of adhesion under dynamic loading are underway [20].

1.1 Catch-Bond Discovery

Binding of natural macromolecules via weak, noncovalent collaboration is basic for living organisms. Catch binding shows one of many interesting and irrational phenomena that emerge in complex biological frameworks. As usually occurs in science, the essential hypothesis was proposed first, and experimental evidence came a lot later. Catch bond was characterized as a bond whose lifetime expanded when it was extended by a mechanical force. Interestingly, life-times of common slip bonds decline during extending. It was commonly expected that most of the natural receptor-ligand interactions are slip bonds [21]. Although, catch bonds have been demonstrated recently. Stream chamber experiments revealed force-improved cell bond in 2002, which could be excused by catch binding between mannose ligands and protein FimH [22]. In 2003 the main complete demonstration with atomic force microscope (AFM) investigates the P-selectin protein, communicated on endothelial cells and platelets, interfacing

with the PSGL-1 ligand communicated on leukocytes. The atomic force microscopy (AFM) experiments demonstrated that beyond a critical value of force, catch bonds carried on as usually slip bonds. The bond lifetime initially increased but finally decreased with developing force [23]. The development and resulting decrease of the binding capacity was likewise seen in stream-chamber that investigates protein FimH mediated connection of microscopic organisms to have cells and beads to surfaces [22]. More as of late, catch-slip behaviour was set up in the actin/myosin complex [24 Functioning of the response of catch bonds evolved in biological conditions. For example, bonds including selectins work in blood flows [21]. Catch binding may stop unconstrained accumulation of streaming leukocytes in fine vessels and postcapillary venules, where forces acting on the bonds are very less [24].

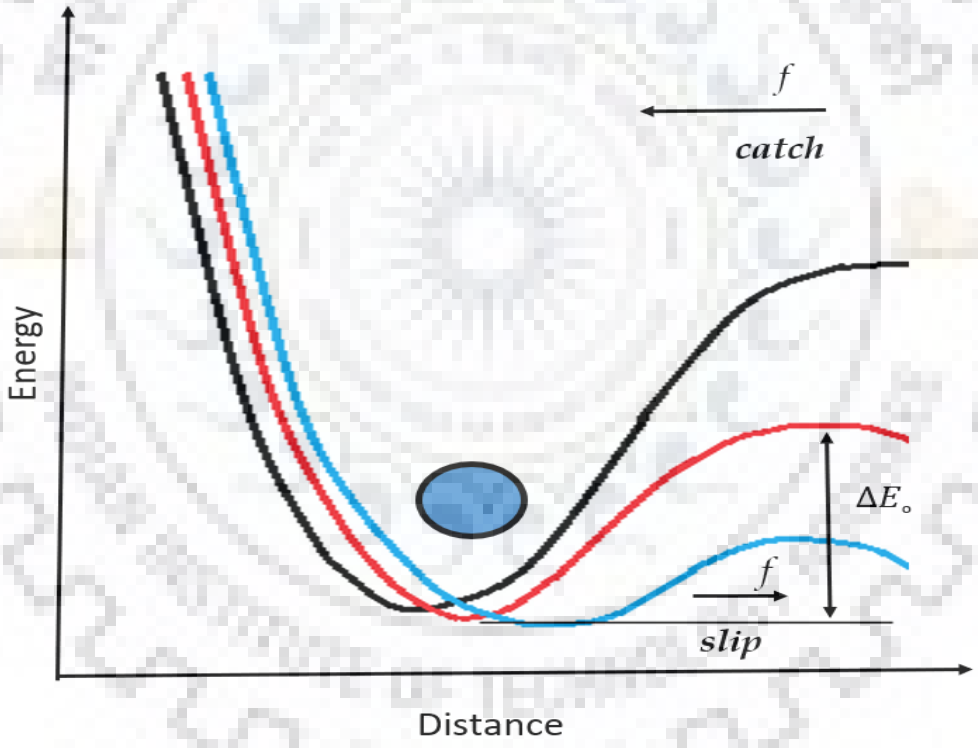

Figure 1.1: Impact of force applied on interaction of ligand-receptor with potential barrier ΔE_0. Force free potential is showed by red lines. Barrier's lowered by force in case of slip binding and favours dissociation of bond. Catch binding happens when force coordinated from barrier in the direction of the minimum raises the barrier.

1.2 Catch and Slip Bonds

For the understanding of force involvement in catch binding at intermolecular level, consideration of interaction energy of receptor-ligand binding is required. Value of barrier height ΔE_0 shows the difference between bound state to unbound state. If the value of ΔE_0 is higher, then bond lifetime will be long. Connected forces *f* initiates straight line changes in the height of barrier ΔE_0 [24]. This circumstances was initially concerned by Bell [25]. The previous circumstances portray slip bonds, since force advances breaking of bonds. In case the free-energy scene of receptor-ligand interaction is like that force pushes the ligand more profound into the receptor, the complex carries on as a catch bond [26]. Eventually, most of the known catch bonds move to slip bonds given adequate force. Large number of clarifications of the catch-slip move have been given in Ref. [26]. A basic depiction is given by two-pathway model [27], which provides both slip and catch mode bond separation. The catch mode contains low energy barrier. By expanding the catch barrier and diminishing the slip barrier, switching from the catch to slip mode are compelled by force. When force are equivalent to the barrier height, bond lifetime has been maximized. Critical exploratory truths can be clarified with a potential involving two bound states and two separation pathways [27]. An elective two-pathway thought is given by the bond separation model [28]. It contends that by changing structure of bond force brings down the potential energy least. Catch binding has been credited to higher-order variance effects that amplify past the Bell mechanism [21]. More complications are given by the force-history reliance of rupture of bond [29].

1.3 Theoretical models

Due to complexity of the problems discussed so far having rupture occurring in real three dimension between many bodies, the system becomes intractable computationally and analytically without making any assumptions. Hence minimalistic models which are simple do not require complex structures and can be used to draw meaningful insights into the basic mechanisms such as physical quantities, scaling behavior, at microscopic level. Mechanical

response of hierarchical systems, cell adhesion and the basic features of friction between two shearing surfaces discussed till now is based on rupture or failure mechanism, caused when an external applied load creates sliding motion between two surfaces. To know the physical behavior of these systems, one dimensional rupture model is used for system modelling [33]. The models usually used for these problems involves two parallel transducers with interlinking bonds which can either rupture or bind uncertainly. Different approaches are adopted to model the influence of mechanical load variation under physiological conditions by applying force on the interconnecting bonds which is distinct for each system under study.

There is possibility of reformation of bonds which is an inherent part of the rupture models. Several attempts had been made in the past to observe microscopic structure physical phenomena using models having rebinding with break of interlinked bonds between force sensors. Friction is the dissipative energy produced due to roughness between sliding contacts having coefficient of friction. The need for friction research arose from the plastic deformation of the sliding bodies and from their surface adhesion [2]. This distinction became the foundation of successful scientific examination into frictional phenomena as shown in studies of Bowden and Tabors on adhesion and plasticity in contacts of metallic surfaces by group of molecular bonds [31]. Pioneering studies made on molecular mechanism of friction by Schallamach led to derivation of a general equation for the frictional force involving average life and the number of the bonds along with the average time lag between breaking and again remaking of a bond at a particular location with the presumption that dynamic friction appear from shearing and then breaking of different bonds between the sliding surfaces. In case of contact between a smooth hard surface and rubber, the bonds are subjected to local molecular adhesion [6]. Recently a model introduced by Filippov et al. is based on relationship between dynamics of rupture and formation of specific bonds and phenomena of macroscopic friction [1]. This model for friction incorporate two rigid plates coupled by bonds which can break spontaneously and then rebind as soon as contact is made under external force. A generalized of this model, by incorporating polymeric flexible transducer that includes rebinding with rupture and where rebinding is governed by the displacement of transducer from its position of equilibrium. As the steady state for displacement of bead is reached problem becomes interesting mathematically. Adhesion phenomena specifically cell adhesion involves rupture and rebinding models. Problem in cell adhesion is multiscale as the molecular activities at the cell material

interface are amplified dramatically on the cell scale [17]. Recent investigations are made on the behavior of distinct adhesion bonds by dynamic force spectroscopy at single molecular level and it is found to be mainly applicable to single bonds, but generally adhesion receptors work cooperatively within clusters [19]. Gaub and coworkers pioneered this field by AFM and later Evans and Ritchie, put forward theoretical approach [32]. Hence, descriptive physical features of forced single adhesion bond have to be expanded to forced cluster adhesion bonds [21]. Rebinding of broken bonds of cluster is also a possibility and to achieve physiological lifetime is critical for adhesion clusters. In case of single bonds, after rupture there is elastic recoil of the force transducer which makes it harder to study rebinding whereas in adhesion clusters broken bonds can rebind till all other bonds remain closed, thus maintaining the closeness required for rebinding. When all the bonds break rebinding becomes impossible as the closeness disappears and the cluster completely disintegrates [30].

Chapter: 2

Model

We develop a rupture model that accounts for relative motion at the single polymer level. In this model system, a one dimensional flexible polymeric transducer is aligned parallel and fixed to an immovable rigid planar substrate by a predefined number of *N* equidistant interlinked bonds. The substrate is rigid and fixed and a persistent force F_T parallel to the transducer is applied, which produces a transducing force on the bonds and therefore called the transducer. There is no role of planar substrate in the rupture dynamics of interlinking bonds. There is vanishingly small distance between the substrate and polymer and so is neglected thus, the model system becomes one dimensional. When the force is applied, the sliding motion of the polymeric transducer begins in x-direction which is parallel to its orientation. The beginning of the sliding motion commences the rupture of the interconnecting bonds between the planar substrate and the transducer, where the process of bond rupture is stochastic.

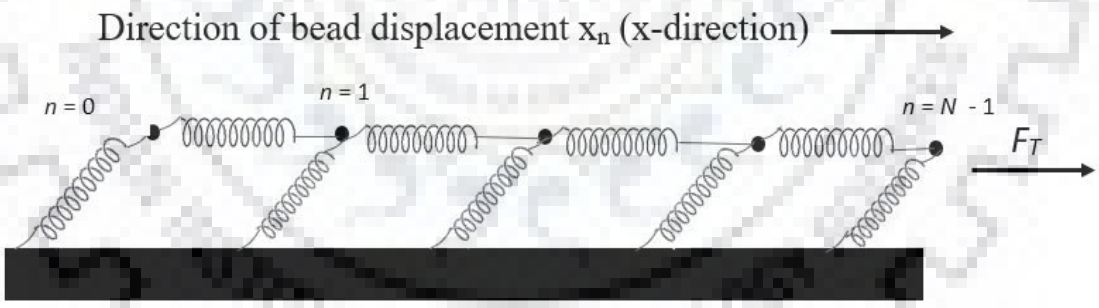

Figure 2.1: A sketch of bead-spring model system

The polymeric transducer is modelled as a bead spring polymer which is defined as a chain of *N* beads connected to each other by harmonic springs having stiffness k_T and bond length at equilibrium is a. All the bonds are modelled as harmonic springs with same equilibrium length a. Discretization of elastic transducer is done such that one bond is connected at each bead and when beads displaces from their equilibrium position $x_{n,0}$ their position is represented by $x_n(t)$ where $n = 0, 1, \ldots, N-1$. This n is the same index as used for the bonds. The bead at $n =$

$N-1$ is acted upon by an external force F_T. The equilibrium position (at time $t = 0$) of initial or zeroth bead at $n = 0$ is $x_{0,0}(0) = 0$ and that of n −th bead is $x_{n,0} = na$. State of a bond is described by a discrete variable q_n, which can assume only two values 0 for open bond or 1 for a closed bond. Rebinding is not taken into account. At time $t = 0$, all bonds are considered closed and displacements of beads from equilibrium positions are zero. Hence, the initial conditions at $t = 0$ are q_n = 1 and $x_n(0)$ = 0. Over time, the transducer starts sliding in the direction of applied force F_T and on each unbroken bond a restoring force $f_n = k_b x_n$ develops opposite to the direction of applied force F_T. On ruptured bond no force develops. The overdamped equation of motion of the beads can be expressed as [33]

$$\gamma \partial_t x_n = k_T \left(x_{n+1} - 2x_n + x_{n-1} \right) - q_n k_b x_n + \delta_{n,N-1} F_T + \zeta_n(t) \tag{2.1}$$

where γ is coefficient of friction for each bead with thermal noise $\langle \zeta_n \rangle$ = 0 following statistics of white noise. $\langle \zeta_m(t) \zeta_n(t') \rangle = 2\, k_B \mathrm{T} \gamma \delta_{m,n} \delta(t - t')$ force applied on the *n*-th close bond is given as $f_n = k_b x_n$. External force F_T is applied only on the bead $n = 0$ which becomes the origin of δ-term. Boundary conditions for free ends can be written as:

$$(x_{-1} - x_0 = 0) \text{ and } (x_{N-1} - x_N = 0)\,. \tag{2.2}$$

Rupture of a bond is modelled, from Kramers theory, as a thermally activated escape over a transition state barrier [21]. Bond dissociation rate which depends on *n* (per unit time probability of transition from closed bond $q_n = 1$ to open bond $q_n = 0$) for slip bond is given by the Bell equation

$$k_{-,n} = k_0 \exp\left[\frac{k_b x_n}{f_b}\right] \tag{2.3}$$

and that for catch bonds is

$$k_{-,n}(f) = k_0 \exp\left[-\frac{\Delta E_d(f) - x_{12} f}{k_B T}\right] \tag{2.4}$$

where, ΔE_d(f) = α $\left[1 - \exp\left(\frac{-f}{f_0}\right)\right]$ is the potential barrier with α being the deformation energy, $f = k_b x_n$ is bond force, and f_0 is saturation force. x_{12} is the barrier width (x_b) and $k_o$is the force free rate constant. On substituting the value of ΔE_d(f) as defined in the expression (2.4) and replace x_{12} by x_b, replace f by $k_b x_n$, and then replacing $\frac{k_B T}{x_b}$ by f_b (the force scale

according to our model) , and taking $\frac{\alpha}{k_B T} = \alpha$ (new constant). Then final expression of rupture rate constant looks like as follow:

$$k_{-,n}(f) = k_0 \exp\left[\frac{k_b x_n}{f_b} - \alpha\left\{1 - \exp\left(-\frac{k_b x_n}{f_0}\right)\right\}\right] \tag{2.5}$$

Modelling bond rupture process as stochastic process, the equation of motion for dynamics of bond is given by

$$q_n(t + \Delta t) = q_n(t) - q_n(t)\theta\left(\alpha_n - \Delta t\, k_{-,n}\right) \tag{2.6}$$

where Δt is a time step, α_n is a random variable belongs (0,1) and θ is the Heaviside step function. The dynamics of bead and bond in above equation of motion totally characterize stochastic model and simulated by standard numerical techniques. We formulate an analytical approach involving mean-field equations (Sec. 2.2).

2.1. Characteristics of Catch Bond

We discuss some readily ascertained characteristics of catch bond. On differentiating Eq. (2.5) with respect to x_n ,

$$\frac{dk_{-,n}}{dx_n} = k_0 \exp\left[\frac{k_b x_n}{f_b} - \alpha\left\{1 - exp\left(-\frac{k_b x_n}{f_0}\right)\right\}\right] \left(\frac{k_b}{f_b} + \alpha \exp\left(-\frac{k_b x_n}{f_0}\right)\left(-\frac{k_b}{f_0}\right)\right) \tag{2.7}$$

For extrema, the following should be satisfied:

$$\frac{dk_{-,n}}{dx_n} = 0,$$

which gives

$$\left(\frac{k_b}{f_b} + \alpha\, exp\left(-\frac{k_b x_n}{f_0}\right)\left(-\frac{k_b}{f_0}\right)\right) = 0$$

and hence

$$\exp\left(-\frac{k_b x_n}{f_0}\right) = \frac{f_0}{\alpha\, f_b}$$

For positive value of minima,

$$\frac{f_0}{\alpha f_b} < 1. \tag{2.8}$$

2.2 Mean Field (MF) Formalism

The equations of motion describing the dynamics of bead and rupture are dependent on the variables $\{x_n\}$ and $\{q_n\}$ denoting distributions of bead positions and bond respectively. The distribution is represented by one single equation as [37]

$$\partial_t p(\{q_n\}, t) = \sum_n (\mathbb{E}_n - 1)\, r_n p + \sum_n (\mathbb{E}_n^{-1} - 1)\, g_n \tag{2.9}$$

where $\mathbb{E}$ is defined by its effect on an arbitrary function as

$$\mathbb{E}\, f(n) = f(n+1) \quad \text{and} \quad \mathbb{E}^{-1} f(n) = f(n-1) \tag{2.10}$$

The transition rates for no rebinding case are for slip bonds is

$$r_n = r(q_n) = q_n k_0\, exp\left[\frac{k_b x_n}{f_b}\right] \tag{2.11}$$

and for catch bonds is

$$r_n = r(q_n) = q_n\, k_0 \exp[(k_b x_n)/f_b - \alpha\{1 - \exp(-(k_b\, x_n)/f_0)\}] \tag{2.12}$$

To account for the stochastic dynamics of polymeric transducer, we need to consider the joint probability $P(\{x_n\}\{q_n\}, t)$ of finding $\{x_n\}$ and $\{q_n\}$ distributions of bead positions and bond variables at time *t*. Fokker Plank equation gives the evolution of this joint probability, which is written as

$$\partial_t P(\{x_n\}\{q_n\}, t) = \sum_n (\mathbb{E}_n - 1)\, r_n P + \sum_n (\mathbb{E}_n^{-1} - 1)\, g_n P - \sum_n [\partial_{x_n} \{\partial_t x_n P\} - D\partial_{x_n}^2 P] \tag{2.10}$$

In the absence of thermal noise $D = 0$, which we assume here, and upon substitution in the above we obtain the full Fokker Plank equation, whose result on solving represent the complete solution of stochastic dynamics.

Mean field approach gives an approximate pathway which leads to deterministic differential equations for the mean values, instead of solving the whole problem as

$$\langle x_n \rangle (t) = \sum_{\{q_n\}} \int d\{x_n\}\, x_n P(\{q_n\},\{x_n\},t) \tag{2.14}$$

$$\langle q_n \rangle (t) = \sum_{\{q_n\}} \int d\{x_n\}\, q_n P(\{q_n\},\{x_n\},t) \tag{2.15}$$

Thus from above, the equations of motion Eq. (2.1) but with force F_T now applied at $n = 0$, within mean-field formalism can be written as

$$\gamma \partial_t \langle x_n \rangle = k_T(\langle x_{n+1} \rangle - 2\langle x_n \rangle + \langle x_{n-1} \rangle) - k_b \langle q_n x_n \rangle + \delta_{n,0} F_T \tag{2.13}$$

Eq. (2.6) for slip bonds is written as

$$\partial_t \langle q_n \rangle = \langle r_n \rangle = -k_0 \langle q_n \, exp\left[\frac{k_b x_n}{f_b}\right] \rangle \tag{2.14}$$

and for catch bond

$$\partial_t \langle q_n \rangle = \langle r_n \rangle = -k_0 \langle q_n \exp\left[\frac{k_b\, x_n}{f_b} - \alpha\left\{1 - \exp\left(-\frac{k_b\, x_n}{f_0}\right)\right\}\right] \rangle \tag{2.15}$$

After neglecting all variable correlations using mean-field approach right hand side of Eqs. (2.13—2.15), we arrive at the following

$$\gamma \partial_t \langle x_n \rangle = k_T(\langle x_{n+1} \rangle - 2\langle x_n \rangle + \langle x_{n-1} \rangle) - k_b \langle q_n \rangle \langle x_n \rangle + \delta_{n,0}\, F_T \tag{2.16}$$

$$= k_T\, \partial_n^2 \langle x_n \rangle - k_b \langle q_n \rangle \langle x_n \rangle + \delta(n) F_T \tag{2.17}$$

for slip bond

$$\partial_t \langle q_n \rangle = \langle r_n \rangle = -k_0 \langle q_n \rangle \exp[(k_b \langle x_n \rangle)/f_b] \tag{2.18}$$

and for catch bond

$$\partial_t \langle q_n \rangle = \langle r_n \rangle = -k_0 \langle q_n \rangle \, exp\left[\frac{k_b \langle x_n \rangle}{f_b} - \alpha\left\{1 - exp\left(-\frac{k_b \langle x_n \rangle}{f_0}\right)\right\}\right] \tag{2.19}$$

Eq. (2.17) is written in the continuum chain limit (assuming bead index *n* as continuous variable. In this limit the boundary condition at free ends becomes

$$\partial_n \langle x_n \rangle |_{n=0} = 0 \text{ and } \partial_n \langle x_n \rangle |_{n=N} = 0. \tag{2.20}$$

The above two equations are partial differential equations with coupling and Eq. (2.19) is the Neumann boundary condition for $\langle x_n \rangle$. The exact solution of the above coupled partial differential equations Eqs. (2.16—2.20) are not possible. So these equations are solved numerically by standard techniques.

2.3 Numerical methods

In order to find the solutions of partial differential equations with their boundary conditions (Eqs. (2.16—2.20)), numerical integration method is used. As an initial step, these equations are first solved by Euler's method keeping time step fixed, but it gave time-step dependent results. To avoid any fixed timestep bias, and to find better solution, adaptive size algorithm is merged with Runge-Kutta second and fourth order methods. Calculations of only fourth order Runge-Kutta are performed and the corresponding results are reported. The adaptive step size is found out to be of $O(10^{-4})$ whose value of tolerance is fixed at 0.0001 or 0.00001. All the calculations are done taking tolerance value to be 0.00001, as it is observed that the results do not significantly improve upon lowering the tolerance value. Modification of step sizes is done with the help of a formula that requires minimal computational time $h_0 = h_1 \sqrt{|\Delta_0/\Delta_1|}$ where Δ_0 is the anticipated accuracy (in terms of tolerance value) and h_1 is the present value of error. h_0 is the assessed step size from the recent step size h_1 for achieving anticipated accuracy. Higher accuracy can be obtained using the formulas that exist in literatures, but by that the adaptive step size gets reduced by one order lacking any considerable change in the results.

I attempted few analytical techniques already stated in Ref. [7], and another standard technique based on Laplace transforms to solve ordinary partial differential equations. It's still in very preliminary stage and hence in relegated to the Appendix.

Chapter: 3

Results and Discussion

In this thesis all parameter units are simulation units in our results. According to physical conditions of experiments, suitable dimensionless parameters combination can often be ascertained [7]. Experimental set up, specifically tailored to measure the quantities that turn out interesting like rupture fronts (not discussed) are required, which arise from the analysis discussed in this thesis. Before we start discussing stochastic simulation results in detail, its informative to look into the characteristics of catch bond compared to slip bonds.

Fig. 3.1 shows the rupture functions ($k_{-,n}$) for slip bond (Eq. (2.3)) as a function of x_n at fixed values of k_b, k_0, and f_b. The characteristics is as expected for an exponential function.

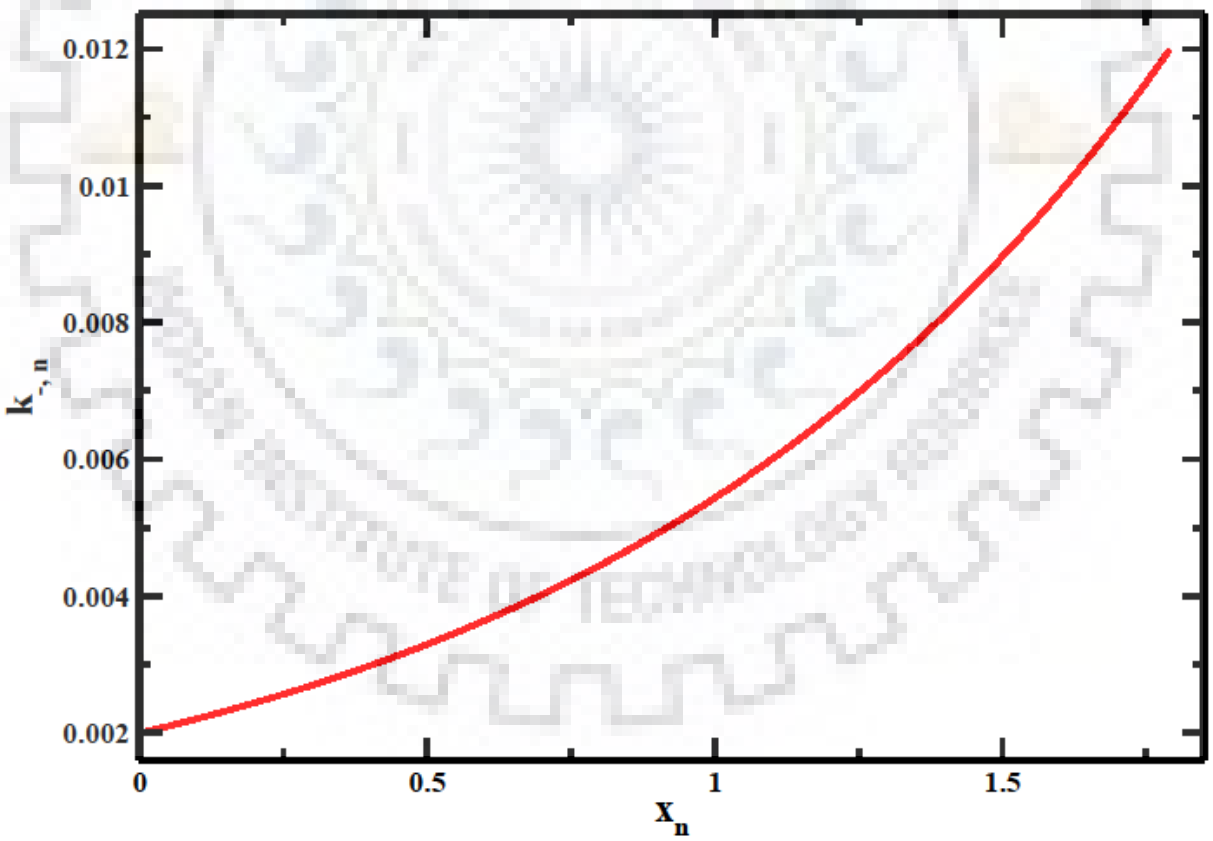

Figure 3.1: Rupture function $k_{-,n}$ representative of slip bond (Eq. (2.3)) as function of x_n for at fixed values of parameters k_b = 1.0, k_0 = 0.002, f_b = 1.0.

Fig. (3.2) shows $k_{-,n}$ for catch bonds in Eq. (2.5) as a function of x_n at fixed values of k_b, k_0, α, f_b, and f_0. There is additional two parameters on which the rupture function depends on, and thus extra terms compared to slip bonds. As noted already in Chapter 2, section 2.1.1, this leads to a extrema condition (Eq. (2.8)), which is a minima and this results due to the fact that catch bonds resist to rupture on applied force and beyond this condition (Eq. (2.8)), it behaves as a slip bond. This characteristic feature of catch bond delays the rupture process as will be shown in stochastic simulation results (next section).

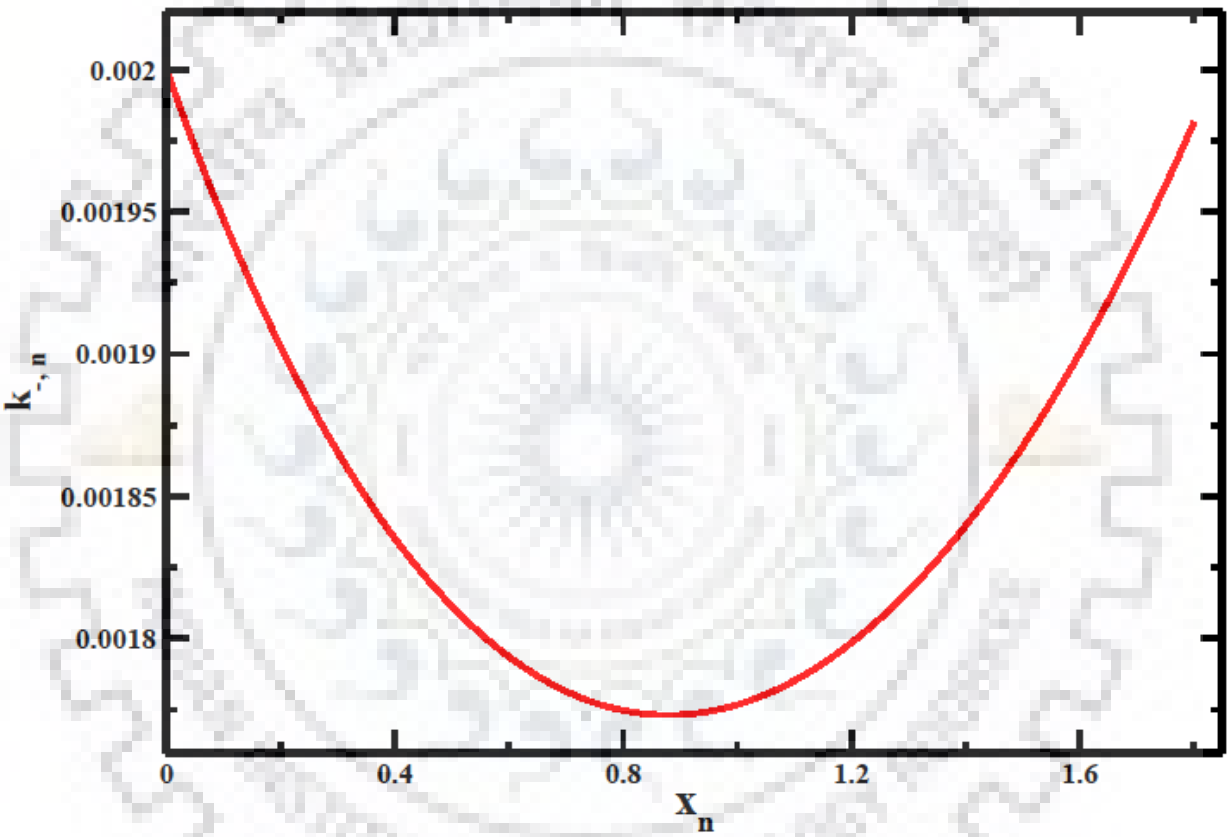

Figure 3.2: Rupture function $k_{-,n}$ representative of catch bond (Eq. (2.5)) as function of x_n for at fixed values of parameters k_b = 1.0, k_0 = 0.002, f_b = 1.0, α = 3.0 and f_0 = 2.5.

3.1 Stochastic Simulation Results

Polymeric model system is simulated as a function of size of polymer *N*, stiffness of polymeric transducer k_T , rupture rate of zero force k_0 , critical force f_b , saturation force f_0 , constant related to deformation energy α , interconnecting bond stiffness k_b , coefficient of friction γ ,

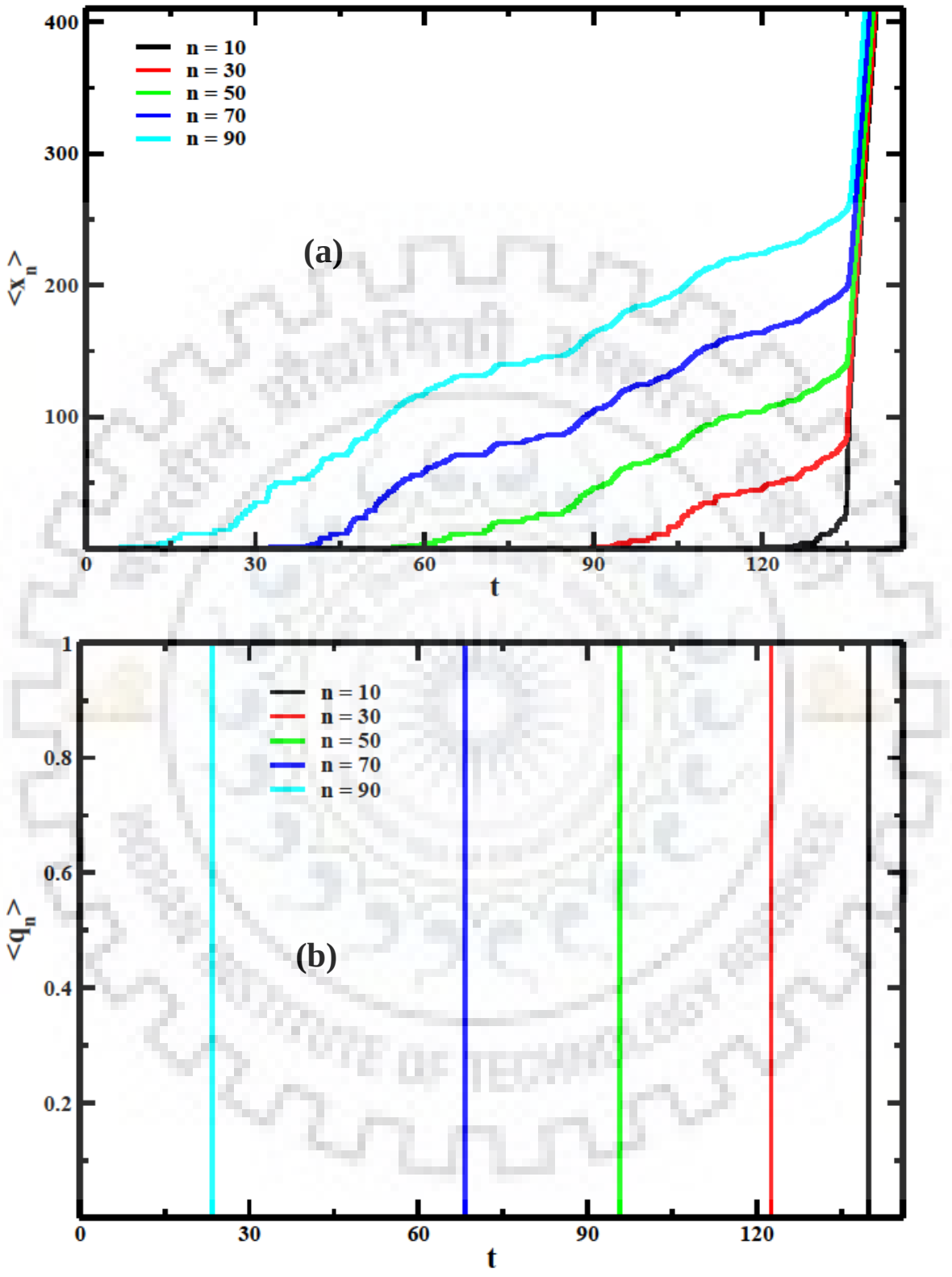

Figure 3.3: (a) $\langle x_n \rangle$ and (b) $\langle q_n \rangle$ as a function of time, from stochastic simulations, at fixed N = 100, k_T = 10.0, k_b = 1.0, F_T = 30.0, γ = 0.005, k_0 = 0.002, f_b = 1.0, α = 3.0, and f_0 = 2.5, for different values of n (= 10, 30, 50, 70, and 90).

number of bead n, constant force applied on the $(N-1)$ −th bond F_T and time t. Stochastic simulation results are averaged over many runs. By using adaptive step size algorithm with Runge-Kutta fourth order, integration has been done, so that bias fixed Δt could be removed as seen within the Euler method.

In Figure (3.3a), $\langle x_n \rangle$ from stochastic simulations is shown as a function of time for different bead index n values at constant force F_T=30. Higher n indicates bead position in close proximity from $(N-1)$ −th bead where F_T is applied. Hence as expected interconnecting bonds nearer to the $(N-1)$−th bead ruptures first than the furthest ones. The corresponding $\langle q_n \rangle$ profiles are shown in Fig. (3.3b) and can be explained as for $\langle x_n \rangle$. Similar results can be seen for different bead index on applying different external forces. Result for different applied external forces on bead index has been shown in Figures 3.4 to 3.7. From these figures it can also be seen that on a same bead index, for higher values of F_T, bond dissociate earlier in time compared to smaller values of F_T.

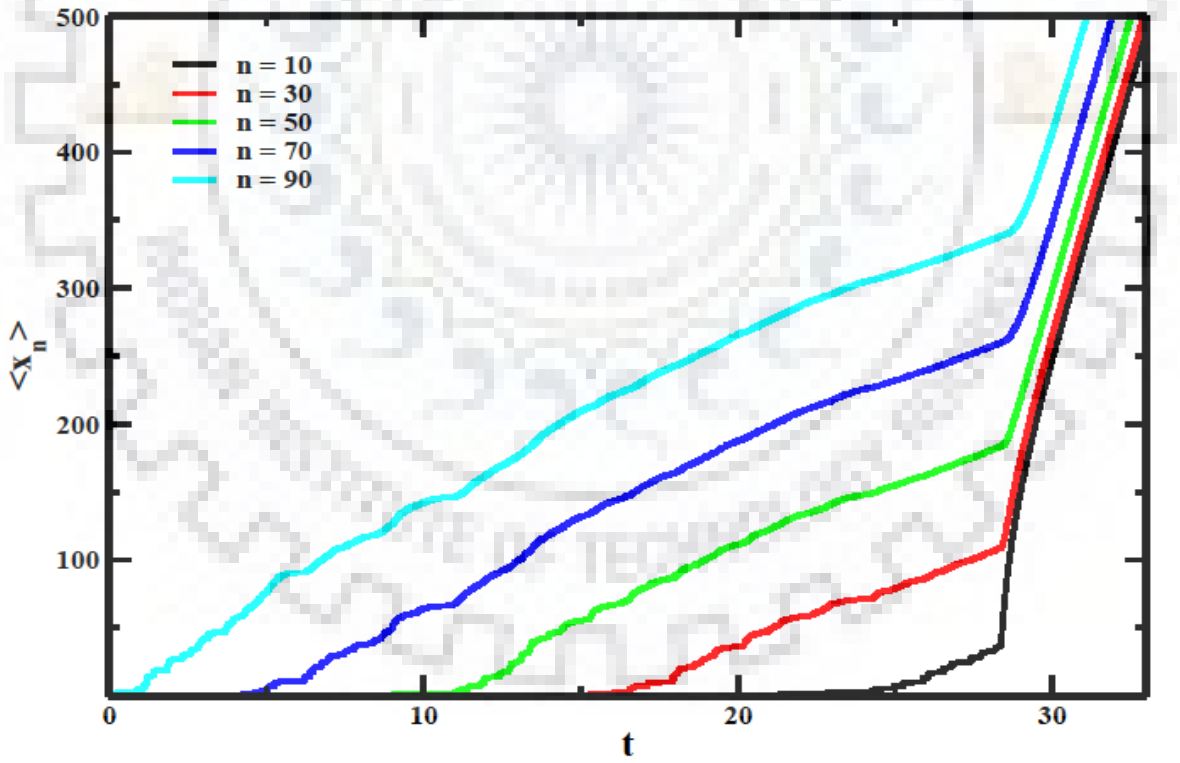

Figure 3.4: $\langle x_n \rangle$ as a function of time, from stochastic simulations, at fixed N = 100, k_T = 10.0, k_b = 1.0, F_T = 40.0, γ = 0.005, k_0 = 0.002, f_b = 1.0, α = 3.0, and f_0 = 2.5, for different values of n (= 10, 30, 50, 70, and 90).

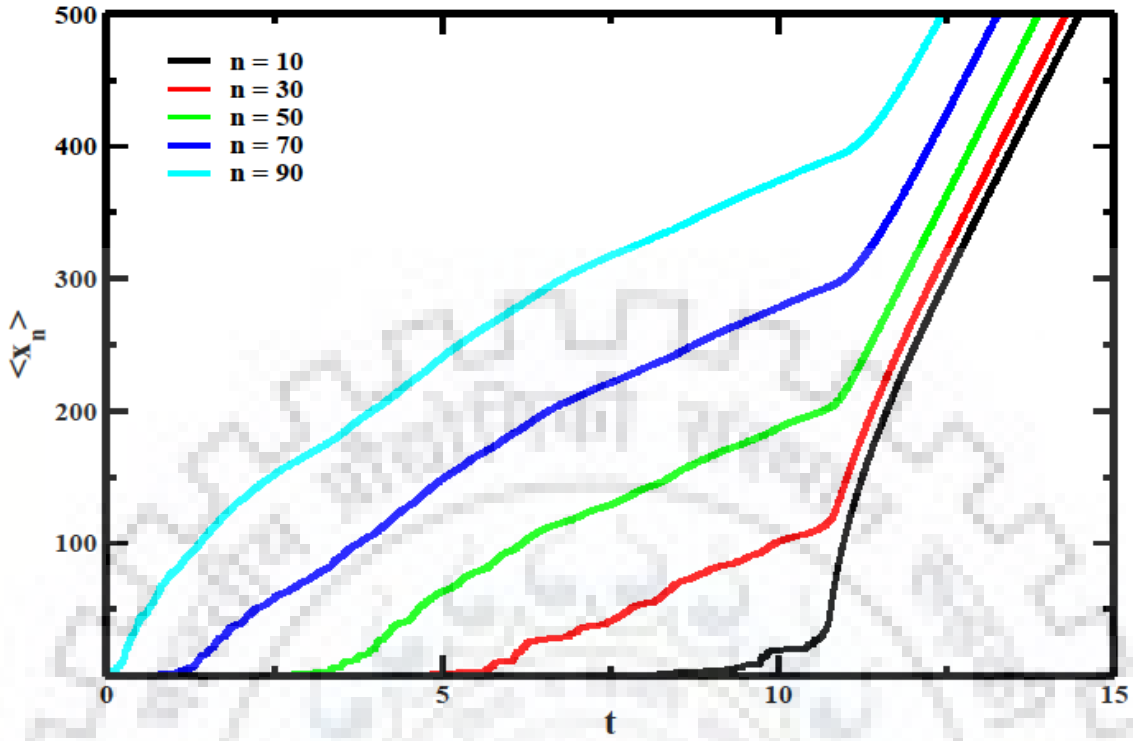

Figure 3.5: $\langle x_n \rangle$ as a function of time, from stochastic simulations, at fixed N = 100, k_T = 10.0, k_b = 1.0, F_T = 50.0, γ = 0.005, k_0 = 0.002, f_b = 1.0, α = 3.0, and f_0 = 2.5, for different values of n (= 10, 30, 50, 70, and 90).

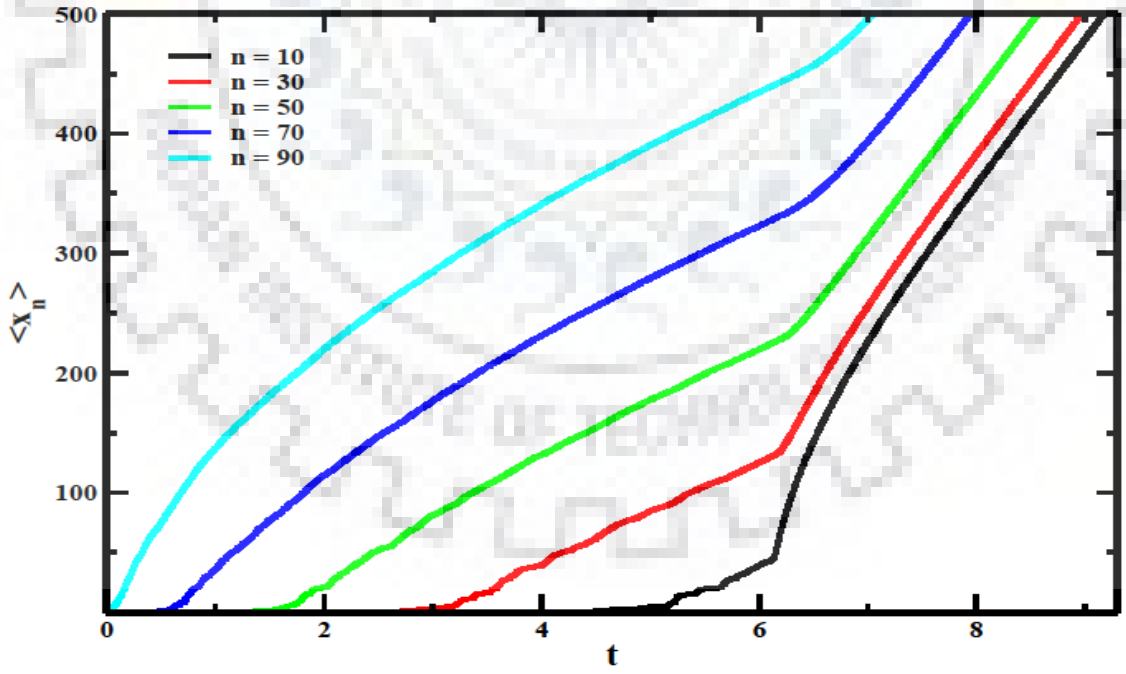

Figure 3.6: $\langle x_n \rangle$ as a function of time, from stochastic simulations, at fixed N = 100, k_T = 10.0, k_b = 1.0, F_T = 60.0, γ = 0.005, k_0 = 0.002, f_b = 1.0, α = 3.0, and f_0 = 2.5, for different values of n (= 10, 30, 50, 70, and 90).

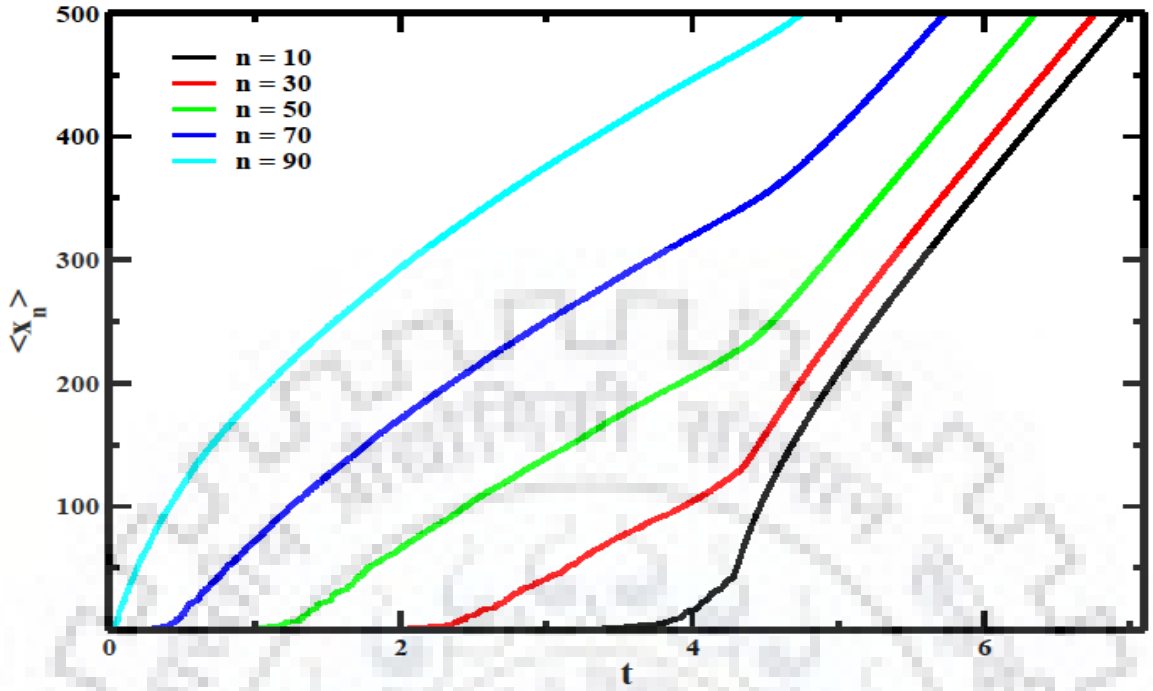

Figure 3.7: $\langle x_n \rangle$ as a function of time, from stochastic simulations, at fixed N = 100, k_T = 10.0, k_b = 1.0, F_T = 70.0, γ = 0.005, k_0 = 0.002, f_b = 1.0, α = 3.0, and f_0 = 2.5, for different values of n (= 10, 30, 50, 70, and 90).

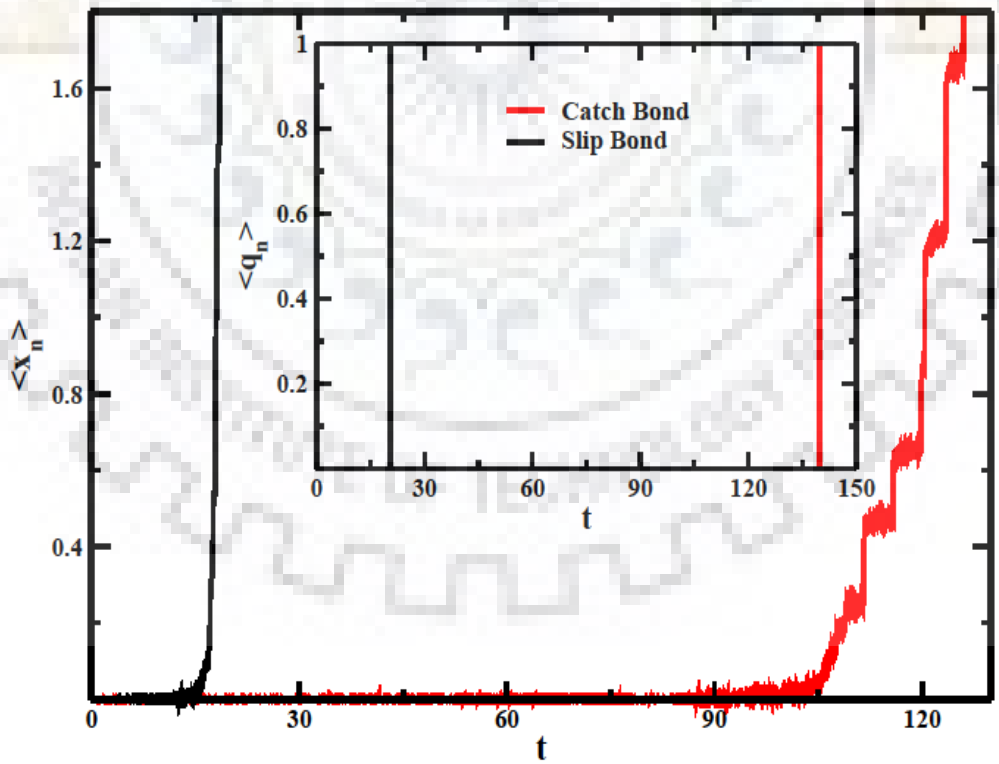

Figure 3.8: Comparison of $\langle x_n \rangle$ and $\langle q_n \rangle$ (inset) for catch and slip bonds as a function of time, from stochastic simulations at fixed N = 100, n = 10, k_T = 10.0, k_b = 1.0, F_T = 30.0, γ = 0.005, k_0 = 0.002, f_b = 1.0, α = 3.0, and f_0 = 2.5.

Figure 3.8 shows the comparison of $\langle x_n \rangle$ and $\langle q_n \rangle$ for catch and slip bond for the same parameters. As the property of catch bond, bond initially resist the breaking that is why bond dissociates later as compare to slip bond (see also above) which can be seen in both $\langle x_n \rangle$ and $\langle q_n \rangle$ profiles. Slip bond dissociates before t = 30 and catch bond dissociates after t = 120.

In Figure 3.9 effect of force F_T on the mean displacement $\langle x_n \rangle$ has been shown. For different value of F_T like 30, 40, 50, 60 and 70. For higher values of F_T bond dissociates early in comparison to low values. Inset curves show the corresponding $\langle q_n \rangle$ from stochastic simulations.

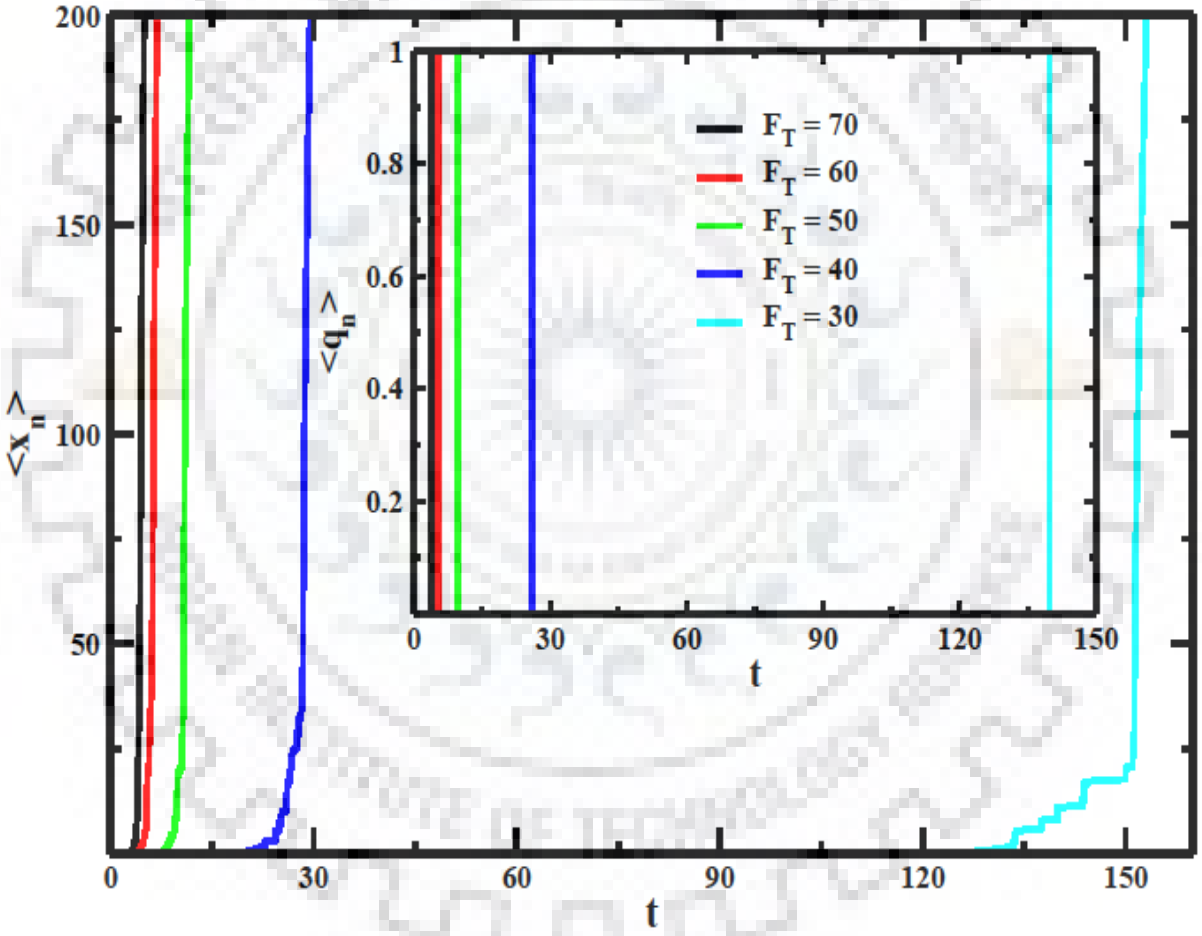

Figure 3.9: $\langle x_n \rangle$ and $\langle q_n \rangle$ (inset) as a function of time, from stochastic simulations, at different values of F_T, for fixed values of N = 100, n = 10, k_T = 10.0, k_b = 1.0, γ = 0.005, k_0 = 0.002 , f_b = 1.0, α = 3.0, and f_0 = 2.5.

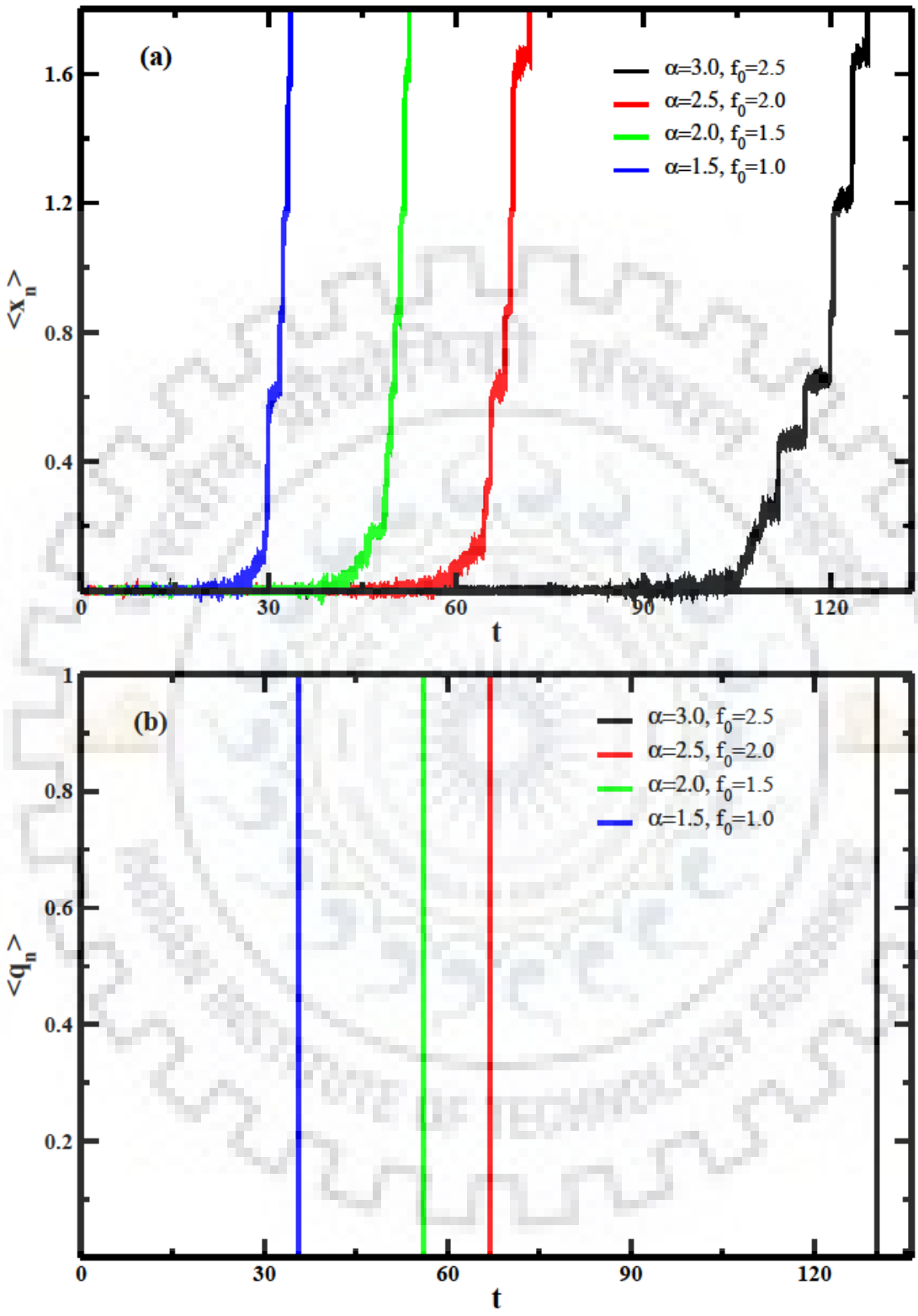

Figure 3.10: (a) $\langle x_n \rangle$ and (b) $\langle q_n \rangle$ as a function of time, from stochastic simulation, at different values of α & f_0 for fixed values of N = 100, n = 10, k_T = 10.0, k_b = 1.0, γ = 0.005, F_T = 30.0, k_0 = 0.002 and f_b = 1.0.

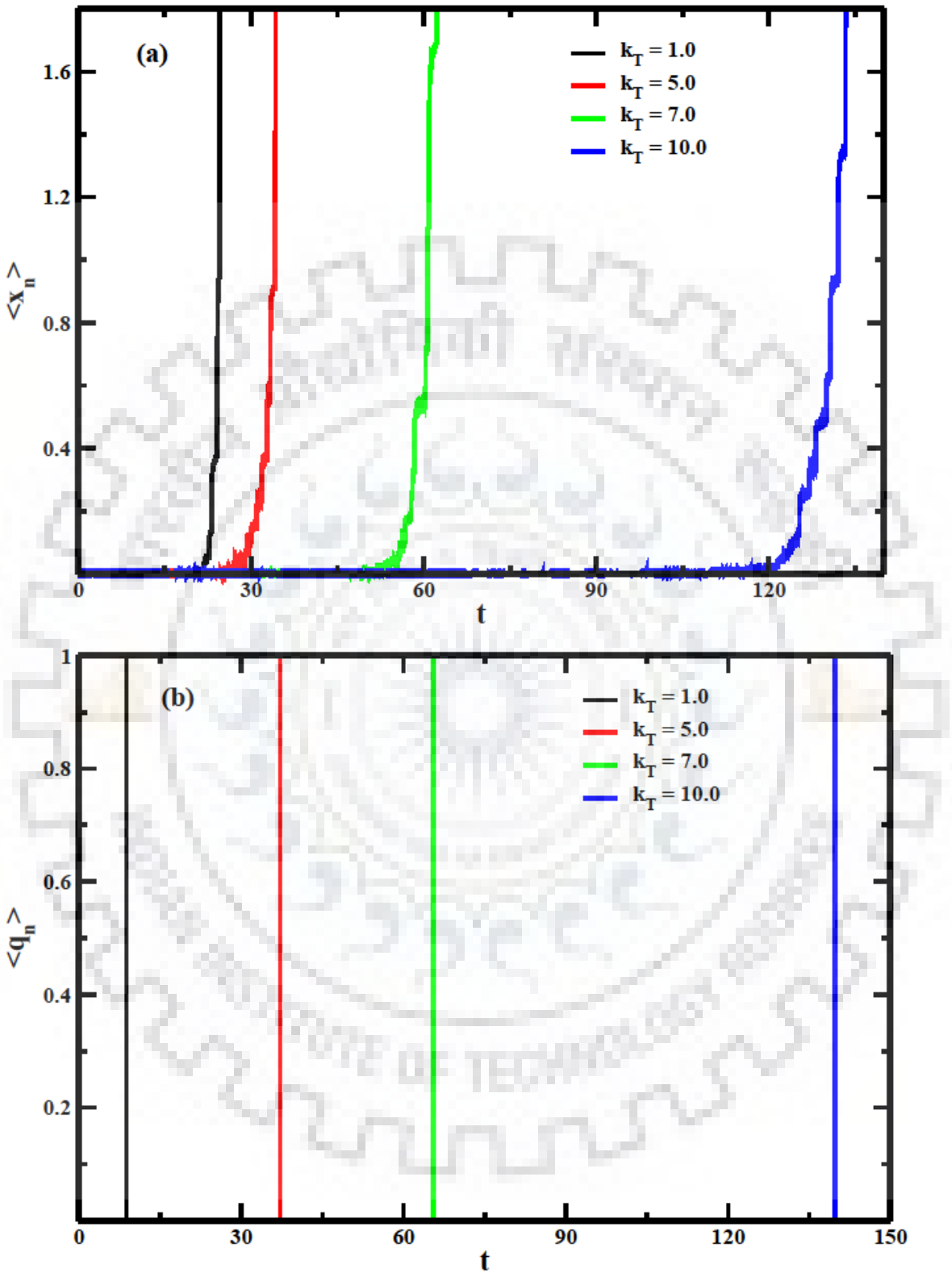

Figure 3.11: $\langle x_n \rangle$ and (b) $\langle q_n \rangle$ as a function of time, from stochastic simulation, at different values of k_T for fixed values of N = 100, n = 10, k_b = 1.0, γ = 0.005, F_T = 30.0, k_0 = 0.002, f_b = 1.0, α = 3.0 and f_0 = 2.5.

Figure. 3.10 (a and b) show the effect of deformation energy term α and saturation force f_0 on $\langle x_n \rangle$ and (b) $\langle q_n \rangle$, as a function of time, respectively, from stochastic simulation results. Deformation energy is defined as the minimum energy required to break the bond and saturation force is defined as the force after which the bond will surely break. As the value of α and f_0 increases simultaneously, bond dissociates later in time as shown in these figures or in other words, the bond rupture time or bond lifetime is higher for higher values of α and f_0.

In Figure. 3.11 we have shown the effect of polymeric transducer stiffness k_T on (a) bead displacement $\langle x_n \rangle$ and (b) $\langle q_n \rangle$, as a function of time. As the value of k_T increases, individual bond rupture time increases.

Chapter: 4

Summary and Conclusion

In summary, we investigated ways to evaluate the coupled partial differential equation of bead and bond dynamics appeared in rupture model framework, both analytically and numerically. In stochastic simulation, our focus was on the new features that arise due to the involvement of catch bonds. To obtain analytic knowhow about the underlying mechanism, mean-field approximations were formulated. Because of coupled dynamics of bead and bond, an exact solution of the mean-field equations is not obtained. Numerical results from stochastic simulations show steady states (sometimes many intermittent ones, see Figure (3.8, 3.10a and 3.11a) for $\langle x_n \rangle$ and same more transient ones can be concluded for $\langle q_n \rangle$ also, which appears not so explicit at the time scale of the corresponding subfigures in (b). A confirmation of such transient steady states requires further investigation, a future scope of this thesis. This steady states are very interesting mathematically, and in physical perspective, they prevent the detachment of two interconnected plates and thus a study may provide useful insights into the modelled system stability. In this thesis, preliminary analytical results, and numerical results which requires further investigation, has been presented. The formalism created may be extended to an array of transducers at a controllable level of tractability (analytical and numerical). Such type of generalization would address deformation response at microscopic level from biological structures and usually from flexible material under loading.

Appendix

Analytical Methods

Exact solution of coupled partial differential equation with Neumann boundary condition are not possible. However, the equations can be made analytically tractable under certain conditions as we discuss in the following methods.

A.I. Method based on Laplace Transforms

We attempt to solve this partial differential equations Eqs. (2.17—2.20) under limiting conditions. We look first into the stationary solution for bead displacement when q_n = 1, these are timescales when bead and bond coupling is yet to set up, then partial differential equation for bead displacement becomes:

$$\gamma \frac{\partial \langle x_n \rangle}{\partial t} = k_T \frac{\partial^2 \langle x_n \rangle}{\partial n^2} - k_b \langle x_n \rangle + \delta(n) F_T \qquad (A.1)$$

for simplification we define new set of variables *x*, *a*, *b*, *d* and *y*

$$\langle x_n \rangle \equiv x, \frac{k_T}{\gamma} \equiv a, \frac{k_b}{\gamma} \equiv b, \frac{F_T}{\gamma} \equiv d, n \equiv y \qquad (A.2)$$

then Eq. (3.1) becomes

$$\frac{\partial x}{\partial t} = a \frac{\partial^2 x}{\partial y^2} - bx + d\delta(y) \qquad (A.3)$$

here x is function of t and y both: $x(t, y)$ with boundary conditions

$$x(0, y) = 0, \frac{\partial x}{\partial y} = 0 \; at \; y = 0, \frac{\partial x}{\partial y} = 0 \; at \; y = N \qquad (A.4)$$

After taking Laplace transformation of equation

$$\frac{dX}{dt}(t, s) = as^2 X(t, s) - sx(t, 0) - x_y(t, 0) - bX(t, s) + d \qquad (A.5)$$

and on applying boundary conditions, the above equation becomes

$$\frac{dX}{dt}(t,s) - (as^2 - b)X(t,s) = d \qquad (A.6)$$

Eq. (A.6) is a constant coefficient first order linear ordinary differential equation. We solve it by finding integration factor (I.F)

$$I.F. = e^{-\int (as^2-b)dt} = e^{-(as^2-b)t}$$

Thus, we have

$$\frac{d}{dt}\left[e^{-(as^2-b)t}X(t,s)\right] = e^{-(as^2-b)t}.d \qquad (A.7)$$

On integrating both sides

$$X(t,s) = e^{(as^2-b)t}\left(\int_0^t e^{-(as^2-b)t}.ddr\right) + C.e^{(as^2-b)t} \qquad (A.8)$$

where, *C* is a constant

On integration by parts Eq. (A.8) becomes

$$X(t,s) = \frac{-d}{(as^2 - b)} + C.e^{(as^2-b)t} \qquad (A.9)$$

By using boundary conditions $X(0,s) = 0$, the constant *C* is obtained as

$$C = \frac{d}{(as^2 - b)} \qquad (A.10)$$

Thus, we have

$$X(t,s) = \frac{de^{(as^2-b)t}}{(as^2 - b)} - \frac{d}{(as^2 - b)} \qquad (A.11)$$

Taking the inverse Laplace transformation of Eq. A.11 we have

$$x(t,y) = \frac{d}{\sqrt{ab}}\left[H(y-t)sinh\sqrt{\frac{b}{a}}(y-t) - sinh\sqrt{\frac{b}{a}}y\right] \qquad (A.12)$$

where *H* is a Heaviside function.

On replacing the original variables as Eqs. (2.16—20), from Eq. (A.2), the solution is

$$\langle x_n \rangle = \frac{F_T}{\sqrt{k_T k_b}} \left[H(n-t) sinh \sqrt{\frac{k_b}{k_T}} (n-t) - sinh \sqrt{\frac{k_b}{k_T}} n \right] \quad (A.13)$$

The result in Eq. (A.13), has to be rigorously tested for its applicability.

A.II Steady state solution using Green's function method

At steady state, at q_n = 1, Eq. (2.17) can be written as:

$$k_T \partial_n^2 \langle x_n \rangle - k_b \langle x_n \rangle + \delta(n) F_T = 0 \quad (A.14)$$

with boundary conditions $\partial_n \langle x_n \rangle |_{n=0} = 0$ and $\partial_n \langle x_n \rangle |_{n=N} = 0$.

Let $k = \sqrt{\frac{k_b}{k_T}}$ and on substituting it in Eq. (A.14), one obtains

$$-(\partial_n^2 - k^2) \langle x_n \rangle = \frac{\delta(n) F_T}{k_T} \quad (A.15)$$

In terms of eigenfunctions of $-\nabla^2$ subjected to the same homogeneous boundary conditions ($-\nabla^2 \Phi_p = k_p^2 \Phi_p$). By using green function method the solution of above equation will be

$$-(\partial_n^2 - k^2) G_k(n \mid n') = \delta(n - n') \quad (A.16)$$

$$G_k(n \mid n') = \sum_p \frac{\Phi_p^*(n') \Phi_p(n)}{k^2 + k_p^2} \quad (A.17)$$

On applying Neumann boundary conditions,

$$\Phi'(0) = 0 = \Phi'(N), \Phi_p = \left(\frac{1}{N}\right)^{1/2} if\ p = 0, \Phi_p = \left(\frac{2}{N}\right)^{1/2} cos\left(\frac{p\pi n}{N}\right) \text{ for } p = 1,2,3, \ldots..$$

$$G_k(n \mid n') = \frac{\frac{1}{N}\left\{1 + 2\sum_{p=1}^{\infty} cos\frac{p\pi n'}{N} cos\frac{p\pi n}{N}\right\}}{k^2 + k_p^2}$$

Which on further rearrangement is written as

$$G_k(\ n \mid n'\ ) = \frac{2}{N}\left[\frac{1}{2k^2} + \sum_{p=1}^{\infty} \frac{cos\frac{p\pi n'}{N} cos\frac{p\pi n}{N}}{k^2 + k_p^2}\right] \qquad (A.18)$$

By applying magic rule,

$$\langle x_n \rangle \ = \frac{2F_T}{Nk_T}\left[\frac{1}{2k^2} + \sum_{p=1}^{\infty} \frac{cos\frac{p\pi n}{N}}{k^2 + \left(\frac{p\pi}{N}\right)^2}\right] \qquad (A.19)$$

A.III Steady state solution using Laplace transformation

In the limit $q_n \to 1$, the bead displacement equation Eq. (2.17) is same as Eq. (A.14). At steady state, solutions are obtained by applying $\frac{\partial \langle x_n \rangle}{\partial t} = 0$ to Eq. (A.14), which becomes

$$k_T \frac{\partial^2 \langle x_n \rangle}{\partial n^2} - k_b \langle x_n \rangle + \delta(n) F_T = 0$$

$$\frac{\partial^2 \langle x_n \rangle}{\partial n^2} - \frac{k_b}{k_T} \langle x_n \rangle + \delta(n) \frac{F_T}{k_T} = 0 \qquad (A.20)$$

As before, for simplification we define new variables as

$$\frac{k_b}{k_T} \equiv b, \frac{F_T}{k_T} \equiv d\ , \langle x_n \rangle \equiv x, n \equiv y \qquad (A.21)$$

On substituting Eq. (A.21) in Eq. (A.20) we have

$$\frac{\partial^2 x}{\partial y^2} - bx + d\delta(y) = 0 \qquad (A.22)$$

Applying Laplace transformation to the both sides of Eq. (A.22) one obtains

$$s^2 X(s) - sx(0) - x_y(0) - bX(s) + d = 0 \qquad (A.23)$$

Further applying boundary conditions in Eq. (A.14) one obtains

$$s^2 X(s) - bX(s) + d = 0$$

$$X(s) = \frac{-d}{s^2 - b} \qquad (A.24)$$

On rearranging Eq. (A.24) as following

$$X(s) = -\left(\frac{\sqrt{b}}{s^2 - \left(\sqrt{b}\right)^2}\right)\frac{d}{\sqrt{b}} \qquad (A.25)$$

and taking inverse Laplace transformation of Eq. (A.25) one obtains

$$x = -\frac{d}{\sqrt{b}}\sinh\sqrt{b}y \qquad (A.26)$$

Finally substituting, the origin values of x, d, b and y as in Eq. (A.21), solution in Eq. (A.26) is obtained to be

$$\langle x_n \rangle = -\frac{F_T}{\sqrt{k_b k_T}}\sinh\sqrt{\frac{k_b}{k_T}}n \qquad (A.27)$$

The result in Eq. (A.27), has to be rigorously tested for its applicability.

Table A.1: Steady state result of $\langle x_n \rangle$ as calculated using Laplace transformation

F_T	$n = 10$	$n = 20$	$n = 30$	$n = 40$	$n = 50$
30	111.8517	2646.973	62528.34	1477076.360	34892248.61739
70	260.990	6176.289	145899.911	344652.8872	81415491.96733

A.IV Travelling-wave solution

By using formalism of travelling-wave, we get propagating solution, for our coupled partial differential equations are

$$\gamma\frac{\partial\langle x_n\rangle}{\partial t} = k_T\frac{\partial^2\langle x_n\rangle}{\partial n^2} - k_b\langle x_n\rangle + \delta(n)F_T \qquad (A.28)$$

$$\frac{\partial\langle q_n\rangle}{\partial t} = -k_0\langle q_n\rangle e^{\left\{\frac{k_b\langle x_n\rangle}{f_b} - \alpha\left\{1 - e^{\left(-\frac{k_b\langle x_n\rangle}{f_0}\right)}\right\}\right\}} \qquad (A.29)$$

On substituting, $\langle x_n \rangle = X\big(c(n - vt)\big) = X(\xi)$

$$\langle q_n \rangle = Q\big(c(n - vt)\big) = Q(\xi)$$

$$\xi = c(n - vt) \tag{A.30}$$

we get

$$\frac{\partial \langle x_n \rangle}{\partial t} = \frac{\partial \left(X(\xi)\right)}{\partial t} = \frac{\partial X(\xi)}{\partial \xi} . \frac{\partial \xi}{\partial t} = \frac{\partial X(\xi)}{\partial \xi} . (-cv)$$

$$\frac{\partial \langle x_n \rangle}{\partial n} = \frac{\partial \left(X(\xi)\right)}{\partial n} = \frac{\partial X(\xi)}{\partial \xi} . \frac{\partial \xi}{\partial n} = \frac{\partial X(\xi)}{\partial \xi} . n$$

$$\frac{\partial^2 \langle x_n \rangle}{\partial n^2} = \frac{\partial^2 X(\xi)}{\partial \xi^2} . c^2$$

$$\frac{\partial \langle q_n \rangle}{\partial t} = \frac{\partial \left(Q(\xi)\right)}{\partial t} = \frac{\partial Q(\xi)}{\partial \xi} . \frac{\partial \xi}{\partial t} = \frac{\partial Q(\xi)}{\partial \xi} . (-cv)$$

$$-\gamma cv \frac{dX \quad (\xi)}{d\xi} = k_T c^2 \frac{d^2 X(\xi)}{d\xi^2} - k_b Q(\xi) X(\xi) + c\delta(\xi + cvt) F_T \tag{A.31}$$

$$-cv \frac{dQ(\xi)}{\partial \xi} = -k_0 Q(\xi) e^{\left\{\frac{k_b X(\xi)}{f_b} - \alpha\left\{1 - e^{\left(-\frac{k_b X(\xi)}{f_0}\right)}\right\}\right\}} \tag{A.32}$$

Introducing $Y = tanh(\xi)$, then

$$X(\xi) = X(Y)\,, Q(\xi) = Q(Y)$$

$$\frac{\partial}{\partial n} = c(1 - Y^2) \frac{d}{dY}$$

$$\frac{\partial}{\partial t} = -cv(1 - Y^2) \frac{d}{dY} \tag{A.33}$$

After expanding the delta function,

$$-\gamma cv(1 - Y^2) \frac{dX(Y)}{dY} = c^2 k_T (1 - Y^2) \frac{d}{dY}\left[(1 - Y^2) \frac{dX(Y)}{dY}\right] - k_b Q(Y) X(Y) + cF_T \sum_{m \to \infty} \frac{m}{\sqrt{\pi}} \exp[-(tanh^{-1} Y + cvt)^2 m^2] \tag{A.34}$$

$$-\gamma cv(1-Y^2)\frac{dX(Y)}{dY}$$

$$= c^2K_T(1-Y^2)\frac{d}{dY}\left[(1-Y^2)\frac{dX(Y)}{dY}\right] - k_bQ(Y)X(Y) + cF_T\sum_{m\to\infty}\frac{m}{\sqrt{\pi}}[1$$

$$- m^2(\frac{2}{3}cvtY^3 + Y^2 + 2cvtY + c^2v^2t^2)]$$

$$-vc(1-Y^2)\frac{dQ(Y)}{dY} = -k_0Q(Y)e^{\left\{\frac{k_bX(Y)}{f_b}-\alpha\left\{1-e^{\left(-\frac{k_bX(Y)}{f_0}\right)}\right\}\right\}} \quad (A.35)$$

using approximations,

$$X(\xi)\to\infty\,, Q(\xi)\to 1\; for\; \xi\to+\infty\;\; or\;\; Y\to\;+1\; for\; N\;\to\infty$$

$$Q(\xi)\to 0, for\;\xi\to-\infty\;\; or\; Y\to\;-1. \quad (A.36)$$

Next travelling wave solutions for $\langle x_n\rangle$ and $\langle q_n\rangle$ are to be obtained in the travelling wave formalism as $X(\xi)$ and $Q(\xi)$, respectively.

References

[1] A. E. Filippov, J. Klafter and M. Urbakh, Friction through dynamical formation and rupture of molecular bonds, *Phys. Rev.Lett.,* 2004, **92**, 135503.

[2] J. Blass, M. Albrecht, B. L. Bozna, G. Wenz and R. Bennewitz, Dynamic effect in friction and adhesion through cooperative rupture and formation of supramolecular bonds, *Nanoscale,* 2015, **7** , 7674-7681.

[3] C. E. Orsello, D. A. Lauffenburger and D. A. Hammer, Molecular properties in cell adhesion: a physical and engineering perspective, *Trends Biotechnol.*,2001, **19** , 310 – 316.

[4] M.G. Rozman, M. Urbakh, J. Klafter and F. J. Elmer, Atomic scale friction and different phases of motion of embeded molecular system, *J. Phys. Chem. B,* 1998, **102**, 7924 – 7930.

[5] M. Feldmann, D. Dietzel, A. Tekiel, J. Topple, P. Grutter and A. Schirmeisen, Universal aging mechanism for static and sliding friction of metallic nanoparticles, *Phys. Rev. Lett.*, 2016, **117** , 025502.

[6] A. Schallamach, A theory of dynamic rubber friction, *Wear*, 1963, **6** , 375 – 382.

[7] R. Borah and P. Debnath, Rupture dynamics in model polymer system, *Soft Matter,* 2016, **12** , 4406 – 4417.

[8] B. N. J. Person and A. I. Volokitin, Rubber friction on smooth surfaces, *Eur. Phys. J. E,* 2006, **21** , 69 – 80.

[9] P. Fratzl and R. Weinkamer, Nature's hierarchical materials, *Prog. Mater. Sci.,* 2007, **52**, 1263 – 1334.

[10] J. W. Dunlop and P. Fratzl, Multilevel architectures in natural materials, *Scr. Mater.*, 2013, **68** , 8 -12.

[11] J. Keckes, I. Burgert, K. Fruhmann, M. Muller, K. Kolln, M. Hamilton, M. Burghammer, S. V. Roth, S. Stanzl-Tschegg and P. Fratzl, Cell-wall recovery after irreversible deformation of wood, *Nat. Mater.*, 2003, **2** , 810 – 813.

[12] J. W. Dunlop and P. Fratzl, Biological composites, *Annu. Rev. Mater. Res.*, 2010, **40** , 1– 24.

[13] F. Barthelat, Z. Yin and M. J. Buehler, Structure and mechanics of interfaces in biological materials, *Nat. Rev. Mater.*, 2016, **1** , 16007, and references therein.

[14] J. B. Thompson, J. H. Kindt, B. Drake, H. G. Hansma, D. E. Morse and P. K. Hansma, Bone indentation recovery time correlates with bond reforming time, *Nature*,2001, **414**, 773-776.

[15] H. Gao, B. Ji, M. J. Buehler and H. Yao, Flaw tolerant bulk and surface nanostructures of biological system, *Mech. Chem. Biosyst*, 2004, **1**, 37 – 52.

[16] V. Gupta, Rupture of multiple receptor-ligand bonds: Bimodal distribution of bond rupture force, *Eur. Phys. J. E*, 2012, **35** , 94.

[17] U. S. Schwarz and S. A. Safran, Physics of adherent cells, *Rev.Mod. Phys.*, 2013, **85**, 1327-1381.

[18] U. Seifert, Rupture of multiple parallel molecular bonds under dynamic loading, *Phys. Rev. Lett.*, 2000, **84**, 2750-2753.

[19] L. Li, H. Yao and J. Wang, Dynamic strength of molecular bond clusters under displacement- and force-controlled loading conditions, *J. Appl. Mech.*, 2015, **83**, 021004.

[20] R. W. Friddle, Analytic descriptions of stochastic bistable system under force ramp, *Phys. Rev. E*, 2016, **93**, 052126.

[21] G. I. Bell, Models for specific adhesion of cells to cells, *Science*, 1978, **200**,618–627.

[22] W. E. Thomas, E. Trintchina, M. Forero, V. Vogel and E. V. Sokurenko, Bacterial adhesion to target cells enhanced by shear force, *Cell*, 2002, **109**, 913–923.

[23] B. T. Marshall, M. Long, J. W. Piper, T. Yago, R. P. McEver and C. Zhu, Direct observation of catch bonds involving cell-adhesion molecules, *Nature*, 2003, **423**, 190–193.

[24] C. Zhu, J. Z. Lou and R. P. McEver, Catch bonds: Physical models, structural bases, biological function and rheological relevance, *Biorheology* 2005, **42**, 443–462.

[25] V. Barsegov and D. Thirumalai, Dynamics of unbinding of cell adhesion molecules: Transition from catch to slip bonds, *Proc. Natl. Acad. Sci. U.S.A*, 2005, **102**, 1835–1839.

[26] V. Pereverzev, O. V. Prezhdo, M. Forero, E. V. Sokurenko and W. E. Thomas, The two-pathway model for the catch-slip transition in biological adhesion, *Biophys. J*, 2005, **89**, 1446–1454.

[27] P. Aprikian, V. Tchesnokova, B. Kidd, O. Yakovenko, V. Yarov-Yarovoy, E. Trinchina, V. Vogel, W. Thomas and E. Sokurenko, Interdomain interaction in the FimH adhesin of Escherichia coli regulates the affinity to mannose, *J. Biol. Chem*, 2007, **282**, 23437–23446.

[28] F. Liu, Z. C. Ou-Yang, M. Iwamoto, Dynamic disorder in receptor-ligand forced dissociation experiments, *Phys. Rev. E*, 2006, **73** , 010901.

[29] B. T. Marshall, K. K. Sarangapani, J. H. Lou, R. P. McEver and C. Zhu, Force history dependence of receptor-ligand dissociation, *Biophys. J*, 2005, **88** , 1458–1466.

[30] T. Erdmann and U. S. Schwarz, Stability of adhesion clusters under constant force, *Phys. Rev. Lett.*, 2004, **84**, 2750-2753.

[31] F. P. Bowden and D. Tabor, *The Friction and Lubrication of Solids*, Oxford University Press, New York, 2008.

[32] E. Evans and K. Ritchie, Dynamic strength of molecular adhesion bond , *Biophys. J.*, 1997, **72**, 1541-1555.

[33] M. Doi and S. F. Edwards, *The Theory of Polymer Dynamics*, Clarendon Press, Oxford, 1986.

[34] J. H. Merkin and D. J. Needham, Propagetting reaction-diffusion waves in a simple isothermal quadratic autocatalytic chemical system, *J. Eng. Math.*, 1989, **23**, 343-356.

[35] W. Malfliet and W. Hereman, The tanh method: Exact solution of nonlinear evolution and wave equation, *Phys. Scr.*,1996, **54**, 563-568.

[36] N. G. Van Kampen, *Stochastic Processes in Physics and Chemistry*, Elsevier, Amsterdam, 2007.

[37] R. Burridge and L. Knopoff, Model and theoretical seismicity, *Bull Seismol. Soc. Am.*, 1967, **57**, 341-371.